ELSEVIER

Physica A 303 (2002) 339–356

PHYSICA A

www.elsevier.com/locate/physa

Collective behavior in a chain of van der Pol oscillators with power-law coupling

Sandro E. de S. Pinto, Sergio R. Lopes, Ricardo L. Viana *

Departamento de Física, Universidade Federal do Paraná, 81531-990 Curitiba, Paraná, Brazil

Received 23 August 2001; received in revised form 20 September 2001

Abstract

We consider the synchronization properties of a one-dimensional chain of coupled van der Pol oscillators. The uncoupled oscillators have an attracting limit-cycle with a given normal mode frequency. We introduce a given level of randomness in the normal mode distribution of the oscillators and study the conditions under which the chain synchronizes. The coupling depends on the distance along the lattice in a power-law fashion. There is a frequency synchronization transition as we pass continuously from a global to a local coupling. We observe phase and lag synchronization transition for other coupling regimes. © 2002 Published by Elsevier Science B.V.

PACS: 05.45.Xt

1. Introduction

Lattices of coupled oscillators are useful models of spatially extended systems, in which the local dynamics may be extremely rich, from a single steady state to a fully chaotic behavior [1]. The interplay between spatial and temporal degrees of freedom, due to the coupling between the oscillators, is responsible for non-trivial collective phenomena, like domain formation, traveling waves, defect propagation and so on [2]. One of the most intensively studied of them is the synchronization of coupled oscillators. In the past decade a large number of works dealt with the plethora of synchronization phenomena that have been described in coupled nonlinear systems such as amplitude, phase, frequency, lag, and generalized synchronization [3].

Frequency synchronization is a natural approach to this subject, since in many oscillating systems we are interested in states for which the temporal rates of change of the

* Corresponding author.
E-mail address: viana@fisica.ufpr.br (R.L. Viana).

0378-4371/02/$ - see front matter
PII: S0378-4371(01)00549-0

phases are equal, rather than the phases themselves. This is the case of physical and biological clocks, where the synchronization of their characteristic rhythms is related to the interaction between the clocks and their environment [4]. Limit-cycle oscillators have been extensively used as models of physical and biological clocks, and their synchronization properties have applications in a great variety of natural phenomena, like the flashing behavior of Asian fireflies [5], Josephson junction arrays [6], circadian rhythms, and heartbeat generation [7].

The idea of studying the heartbeat using coupled limit-cycle oscillators dates back from the pioneering works of van der Pol and van der Mark [8]. The underlying principle is that the cardiac rhythms are generated by self-excitatory and subsidiary pacemakers, which are specialized cells that must act in a synchronized way in order to produce coherent behavior [9]. The sinoatrial (SA) and atrioventricular (AV) nodes are such pacemakers, which can be modeled by coupled driven van der Pol (vdP) oscillators [10]. This approach has been used to explain many heartbeat phenomena of interest in clinical practice such as the Wenckebach periodicity, extrasystoles, and pseudo-blocks [11]. In this case, the SA node is regarded as the primary pacemaker and is the primary stimulus for the coupled oscillator system. A description that combines coupled vdP oscillators with nerve pulse equations was proposed to relate the SA and AV nodes with the structures that transmit pulses to the myocardium [12].

It is possible to study frequency synchronization in systems of coupled vdP oscillators even when their dynamics are chaotic, by defining a suitable phase for each of them and considering as a synchronized state the situation in which the temporal rates of phase changes are equal. If the interacting oscillators are in a periodic regime this is also known as mode-locking. If we let the oscillators to be non-identical, for example due to a parameter mismatch which affects the natural frequency of each uncoupled oscillator, it is possible to have synchronization if the coupling effect overcomes this frozen disorder in the system. This is the case of non-local couplings, which consider not only the nearest neighbors of a given oscillator but also other lattice sites.

Non-local oscillator couplings appear in models of assemblies of biological cells with oscillatory activity, when their interactions are mediated by some rapidly diffusing chemical substance [13]. This type of coupling is also possible in certain biological neural networks [14]. Two types of non-local couplings including some effective range have been analyzed: (i) *intermediate range* couplings, considering a finite number of non-nearest neighbors, usually with the same weight [15]; and (ii) *infinite range*, as power-law couplings, in which the interaction strength decays with the lattice distance in a power-law fashion. Intermediate-range couplings have been studied, mainly in the thermodynamic limit [16], whereas power-law couplings have received comparatively less attention. We shall also mention *small-world networks* that have, besides the regular couplings with nearest and non-nearest neighbors, also a small number of randomly chosen non-local connections [17]. The properties of such networks are the object of an intense investigation, including their synchronization behavior [18].

Synchronization in assemblies of locally coupled limit-cycle oscillators has received a great deal of attention in the last years [19,20]. The case of two coupled and randomly driven vdP oscillators was considered by Jensen [21], who has studied the conditions

under which the oscillators synchronize. It was also observed that a chain of locally coupled vdP oscillators can exhibit phase synchronization, and that is possible to control this effect by means of periodic forcing [22]. A prototypic limit-cycle oscillator chain is the Kuramoto model [23], consisting of linear oscillators with a sinusoidal coupling [24]. A non-local version of this model with a coupling strength decaying with the lattice distance in a power-law fashion was considered by Rogers and Wille [25], who studied the frequency synchronization properties of the chain as the effective coupling range was varied.

In this paper, we shall consider a lattice of vdP oscillators with such a coupling prescription, that has also been studied in coupled circle map lattices [26,27]. For a lattice of piecewise linear maps with this coupling, the Lyapunov spectrum was analyzed in terms of the coupling strength and range, as well as the corresponding effects on the amplitude and phase synchronization of maps [28].

If the coupled oscillators were identical, their synchronized state would be a high-dimensional attractor with a large basin of attraction. However, this scenario changes if the oscillators are non-identical due to small differences in their parameters. This is a situation to be expected in physical and biological applications of coupled oscillators [2]. In arrays of coupled Josephson junctions, for example, the fluctuations in the microscopic parameters lead to non-uniformity of the chain [29]. Likewise, in the heartbeat the synchronization of the pacemakers should overcome possible small structural differences in the self-oscillating cells [9]. Nevertheless, the parameter variations for the coupled oscillators have to be chosen in such a way not to alter their basic dynamics.

The normal modes (or natural frequencies) of each oscillator are taken to be non-identical and randomly distributed within a specified interval. The interval bounds are specified so as to always give an attracting limit cycle encircling the origin of the state space, such that a geometrical phase can be defined at every instant for the system. The rate of change of this phase will be identified as the oscillator frequency, and we investigate the phase and frequency synchronization in the chain. We analyze the effects of coupling strength and range, as well as the influence of the lattice size. Phase synchronization can occur, as evidenced by the numerical computation of an order parameter, and some relations between phase, frequency, lag, and amplitude synchronization are discussed.

This work is organized as follows: in Section 2 we introduce the coupled vdP oscillator chain to be studied. Section 3 introduces some diagnostics of frequency synchronization, and discusses the transition between synchronized and non-synchronized states with respect to variations in the coupling parameters. Section 4 deals with phase synchronization in the lattice by using an order parameter. The last section contains our conclusions.

2. Coupled van der Pol oscillators

We shall consider a one-dimensional lattice of vdP oscillators, in which each site has a continuous state variable $x^{(i)}(t) \in \mathscr{R}$, where $i = 1, 2, \ldots, N$. The time evolution of

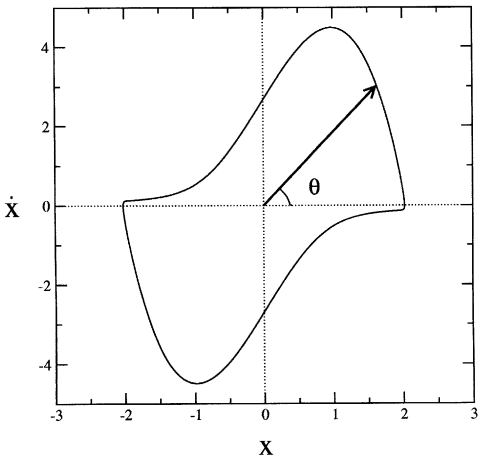

Fig. 1. Phase portrait of an uncoupled vdP oscillator with $a = 2.8$, $b = 1.0$, and $\Omega = 1.0$, showing how the phase is defined for the system.

this variable for each oscillator is governed by the differential equations [12]

$$\frac{\mathrm{d}^2 x^{(i)}}{\mathrm{d}t^2} + a(x^{(i)^2} - b^2)\frac{\mathrm{d}x^{(i)}}{\mathrm{d}t} + \Omega^{(i)} x^{(i)} = 0\,, \tag{1}$$

where $a > 0$ and $b > 0$ are constant parameters, and $\Omega^{(i)}$ are normal mode frequencies which have values within the interval $[0, 1]$. In Fig. 1, we depict a phase portrait for a single vdP oscillator obtained for the following set of values: $a = 2.8$, $b = 1.0$, and $\Omega = 1.0$. The attractor for these parameter values is a stable limit cycle encircling the origin $(x, \dot{x}) = (0, 0)$, in such a way that we can parameterize the dynamics along the limit cycle by means of a geometrical phase $\theta^{(i)} \in [0, 2\pi)$ defined as

$$\tan\theta^{(i)}(t) = \frac{\dot{x}^{(i)}(t)}{x^{(i)}(t)}\,, \tag{2}$$

provided $x^{(i)} \neq 0$ and the origin (that is an unstable fixed point) belongs to the region internal to the limit cycle. In the following, we will fix the values of the parameters a and b and vary the normal mode frequency Ω. For all chosen values of Ω within the $[0, 1]$ interval we are able to define the geometrical phase for the uncoupled oscillators.

The coupling prescription we use in this work includes not only the nearest neighbors of a given oscillator, but all other lattice sites. However, the strength of these non-local interactions depend on the lattice distance in a power-law fashion. The coupled oscillator chain is described by [25]

$$\ddot{x}^{(i)} + a(x^{(i)^2} - b^2)\dot{x}^{(i)} + \Omega^{(i)} x^{(i)}$$

$$= \frac{K}{\eta(\alpha)} \sum_{j=1}^{N'} \left(\frac{1}{j^\alpha}\right) [\sin(x^{(i-j)} - x^{(i)}) + \sin(x^{(i+j)} - x^{(i)})] \tag{3}$$

for $i = 1, 2, \ldots, N$, where $N' = (N-1)/2$, for N odd, and

$$\eta(\alpha) = 2\sum_{j=1}^{N'} \frac{1}{j^{\alpha}} \tag{4}$$

is a normalization factor. $K \geqslant 0$ is the coupling strength and $\alpha \geqslant 0$ is a real parameter expressing the effective range of the interaction between sites. We assume periodic boundary conditions for the lattice, such that we have $x^{(i\pm N)}(t) = x^{(i)}(t)$ for all times.

The right-hand side of Eq. (3) is a weighted average of terms involving non-nearest neighbors, the normalization factor being the sum of the corresponding statistical weights. For $\alpha = 0$ there results $\eta = N - 1$, and we may rewrite the summation in the coupling term of (3) in such a way that we obtain a global type of coupling

$$\ddot{x}^{(i)} + a(x^{(i)^2} - b^2)\dot{x}^{(i)} + \Omega^{(i)}x^{(i)} = \frac{K}{N-1}\sum_{j=1, j\neq i}^{N} \sin(x^{(j)} - x^{(i)})\,, \tag{5}$$

in which each site interacts with the "mean field" caused by the collective influence of the oscillator assembly. In the limit $\alpha \to \infty$ only the terms with $j = 1$ survive in the summations, hence $\eta \to 2$, and just the nearest neighbors contribute to the interactions, resulting in the local coupling

$$\ddot{x}^{(i)} + a(x^{(i)^2} - b^2)\dot{x}^{(i)} + \Omega^{(i)}x^{(i)} = \frac{K}{2}[\sin(x^{(i-1)} - x^{(i)}) + \sin(x^{(i+1)} - x^{(i)})] \tag{6}$$

used in the Kuramoto model [23]. Hence, the power-law coupling (3) is a form of interpolation between these two limiting cases. We will call the coupling forms with $\alpha = 0$ (long range) and large α (short range) as global and local ones, respectively. Further properties of the coupling term in Eq. (3) for arbitrary α may be found in Ref. [26].

3. Frequency synchronization

As we shall address in this paper the frequency synchronization properties of a limit-cycle oscillator chain, we define a perturbed frequency as a mean rate of temporal change of the phase defined by Eq. (2), or

$$w^{(i)} = \lim_{t\to\infty} \frac{\theta^{(i)}(t+T) - \theta^{(i)}(T)}{t} \quad (i = 1, 2, \ldots, N) \tag{7}$$

and T is chosen such that transients have decayed. This frequency is the continuous-time analog of the winding number for unidimensional circle maps. Two or more oscillators are said to be frequency synchronized if their frequencies are, up to a specified tolerance equal to 10^{-5} in our case. If the oscillators are synchronized in frequency this does not mean necessarily that their phases are equal (phase synchronization), the same observation being valid for the state variables x and $\dot{x}$ themselves (amplitude synchronization). However, phase synchronization do imply frequency synchronization, as can be seen from Eq. (7).

If we couple identical vdP oscillators in the absence of noise, the frequency-synchronized state is achieved after a number of transient cycles, since even if each

oscillator starts from a different initial condition it will end up at a stationary state with the same frequency, even though the phases may not be equal at each instant. Hence, in order to see the emergence of interesting collective behavior we have to couple *non-identical* oscillators. This can be achieved by giving a different normal mode frequency $\Omega^{(i)} \in [0,1]$ to each oscillator, randomly chosen according to a Gaussian distribution centered at $\Omega_0 = 1/2$. Once these natural modes are set up in the beginning of numerical simulations, they remain constant.

Considering the time evolution of the phase (2), after an oscillator settles down into a limit cycle, we may gain some insight into the phase dynamics by considering a lattice of coupled sine-circle maps: $\psi \mapsto f(\psi) = \omega + \psi + \kappa \sin(2\pi\psi)$, where $0 \leqslant \psi < 1$ is a normalized angle, $\omega \in [0,1]$, and $\kappa > 0$. In this case, a lattice of non-identical maps may be realized by randomly distributing the natural frequencies ω over their range. In the absence of coupling and for zero nonlinearity ($\kappa = 0$), each map is just a rigid rotation and its winding number is equal to the natural frequency ω. Weak nonlinearity ($\kappa < 1$) causes the appearance of entrainment (mode-locking) and quasiperiodic behavior. The mode-locking regions are sequences of Arnold tongues in the parameter (κ *versus* ω) space corresponding to rational winding numbers m/n [30]. The coupling between maps is equivalent to a fluctuating term added to each map, and may cause the map orbits to exit some Arnold tongue and either entering another one or settling down into a quasiperiodic region, for example. This makes possible for a number of maps to lock their frequencies at a common value and form synchronized clusters.

Likewise, for the chain of continuous-time vdP oscillators in Eq. (3), if we consider the uncoupled ($K = 0$) and linear ($a = 0$) systems we have a phase evolution given by $\theta^{(i)}(t) = \theta^{(i)}(0) + \Omega^{(i)}t$. In this case, the frequencies are equal to the normal modes: $w^{(i)} = \Omega^{(i)}$, yielding periodic (harmonic) or quasiperiodic response if $\Omega^{(i)}$ is rational or irrational, respectively. For $a \neq 0$, the system typically exhibits a limit cycle (as that of Fig. 1) and the frequencies are no longer equal to the normal modes [31]. The coupling between oscillators adds to each of them a time-variable kick that alters their frequencies in a way qualitatively similar to that described above for circle maps.

The process of synchronization, or mode-locking between the coupled non-identical oscillators can be regarded as the adjustment of their frequencies as a result of the interaction. This results from the fact that the Lyapunov exponent of each oscillator is zero in the direction of the flow [30], i.e., the phase dynamics on the limit cycle has marginal stability against perturbations in the same direction of the flow. This allows for small adjustments of the oscillator phases due to the external driving caused by the coupling interactions, even when the amplitudes are behaving chaotically, a fact that has been extensively studied in systems like Rössler oscillators [32,33].

We shall assess the effect of coupling on the synchronization properties of a chain of vdP oscillators with a power-law coupling given by Eq. (3), with random initial conditions $(x^{(i)}(0), \dot{x}^{(i)}(0))$ and periodic boundary conditions. The coupled ordinary differential equations are numerically solved by using a 12th order Adams method (from the LSODA package [34]), and at each time we compute the corresponding phase $\theta^{(i)}(t)$, from which the frequencies $w^{(i)}$ are evaluated using (7). Fig. 2, where the coupling strength was kept constant, displays the perturbed frequencies for the lattice sites at a fixed time, after transients have died out. We present three representative

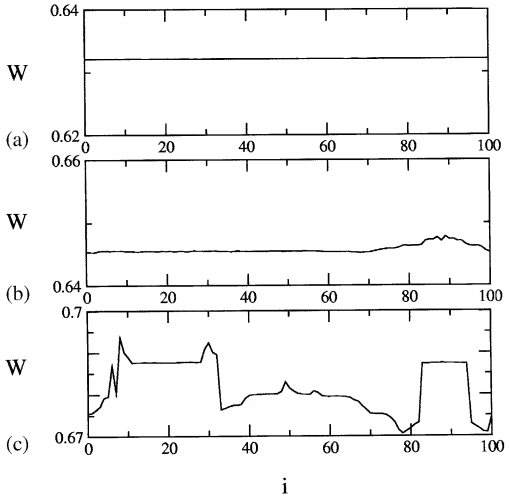

Fig. 2. Frequency profile for a lattice of $N = 101$ coupled vdP oscillators with $a = 2.8$, $b = 1.0$, $K = 3.0$, random initial conditions, periodic boundary conditions, normal mode frequencies randomly distributed over the interval $[0, 1]$. (a) $\alpha = 0.0$; (b) $\alpha = 1.3$; and (c) $\alpha = 1.7$.

cases: for $\alpha = 0$ (global coupling) the entire lattice exhibits frequency synchronization at $w \approx 0.63$ [Fig. 2(a)]. Note that, due to coupling, the average frequency is different from $\frac{1}{2}$, which is the expected average for the randomly chosen normal modes. For intermediate range ($\alpha = 1.3$) we see that most, but not all sites are synchronized [Fig. 2(b)]; and for a slightly higher value ($\alpha = 1.7$) just a small fraction of the lattice sites has synchronized, forming two large plateaus [Fig. 2(c)]. As α continues to grow we have no longer a synchronized state, at least for this coupling strength value.

We introduce, to characterize the synchronized states, the dispersion of the perturbed frequencies with respect to their spatial average $\langle w \rangle = (1/N) \sum_{i=1}^{N} w^{(i)}$, given by the corresponding standard deviation

$$\delta w = \left[\frac{1}{N-1} \sum_{i=1}^{N} (w^{(i)} - \langle w \rangle)^2 \right]^{1/2} . \tag{8}$$

Synchronized oscillators present a very small dispersion, whereas in a completely non-synchronized state it is of the same magnitude as the dispersion of the randomly chosen normal modes. In Fig. 3(a), we fix the coupling strength and vary the range parameter. For low values of the range parameter the dispersion is very small, and as α builds up past a critical value $\alpha_c \approx 1.7$, the dispersion increases abruptly to values one order of magnitude higher. This synchronization transition was described in an extended Kuramoto model [25] and in coupled circle map lattices [26,27].

When α is close to this critical value we typically have coexistence of synchronization plateaus for which the oscillators are synchronized at *different* frequencies. Hence, a simple average may not be representative of the lattice as a whole, so that in addition to the dispersion we also compute the relative average size of the synchronization

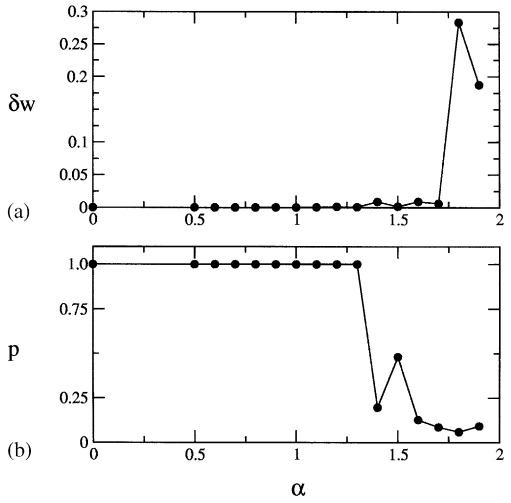

Fig. 3. (a) Frequency dispersion and (b) synchronization degree *versus* coupling range. Other parameters are the same as in Fig. 2.

plateaus [25]. Let N_i be the length of the ith plateau, and N_p the total number of them, with average size $\langle N\rangle = (1/N_p)\sum_{i=1}^{N_p} N_i$. We define a *synchronization degree* p as the ratio between the average plateau length and the total lattice size N, or $p = \langle N\rangle/N$. For a totally synchronized state, as that depicted in Fig. 2(a), we have just one plateau comprising the entire lattice ($\langle N\rangle = N$) so that $p = 1$. On the other hand, for a completely non-synchronized state there are almost as many plateaus as sites, so $N_p \approx N$, or $\langle N\rangle \approx 1$, giving $p \approx 1/N \to 0$ if $N \to \infty$. A quantity similar to the synchronization degree is the frequency-order parameter introduced by Sakaguchi et al. [35]: $E = N_E/N$, where N_E is the number of oscillators in the largest plateau.

Fig. 3(b) illustrates the variation of the synchronization degree with the range parameter for the same parameters we have used when computing the frequency dispersion. The transition exhibited by p is not as sharp as in the previous case, nevertheless the synchronization degree begins to have low values (around 0.1 or less) for $\alpha \approx 1.7$, in accordance with Fig. 3(a). The reason for this difference is the instability of the synchronization degree under small deviations of the frequencies. For example, if there is only one site that refuses to synchronize within an otherwise large plateau, the latter is divided into two pieces and p decreases a large amount, regardless of how much that rebel site deviates from the others. Hence, low values of p do not always imply in a total absence of synchronization. This makes the dispersion a more robust evidence of the synchronization transition as the coupling varies from global to local.

In Fig. 3, the range parameter was varied from zero to a value slightly less than 2.0, since after that the oscillators die out and the phase as well as its corresponding time rate cease to be defined. Other initial conditions, in addition, may cause the oscillators to die out even before this value. This occurs when the limit cycle collapses into

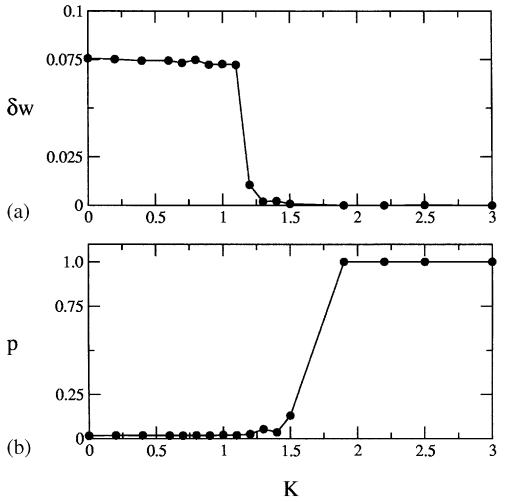

Fig. 4. (a) Frequency dispersion and (b) synchronization degree *versus* coupling strength for a lattice of $N = 101$ vdP oscillators with $\alpha = 0.0$.

a stable fixed point, due to the coupling additive effect. We have verified that the oscillators may even have a rebirth in some circumstances. This oscillator death effect has been previously observed in lattices of coupled limit-cycle oscillators [36].

A similar synchronization transition is observed by fixing the range parameter at $\alpha = 0$ and varying the coupling strength K. In this case, if we depict either the frequency dispersion [Fig. 4(a)] or the synchronization degree [Fig. 4(b)] *versus* K, we see that for weak coupling the lattice is not synchronized, even though we are considering a coupling with long effective range. In the uncoupled case there would be no synchronization at all, and by continuity this is expected to occur for K small enough. The transition to small frequency dispersion presents a critical range about 1.2. This behavior has been described in coupled logistic map lattices and it is related to the Lyapunov exponent spectrum [37].

The dependence of this critical range on the coupling strength K is shown by Fig. 5. For weak coupling the critical range is not defined because the transition from synchronized to non-synchronized states does not occur. After a value of K about 0.9 the critical effective range α_c grows monotonically with the coupling strength. The mean curve resembles a phase transition curve for the para-ferromagnetic transition in spin systems, and in fact such transition has been described for kinetic Ising models [38], when the coupling between spins decreases with the lattice distance as a power-law [39,40].

Another variable that influences the value of the critical range parameter is the lattice size N. In Fig. 6, we present a series of values for α_c in terms of the inverse size $1/N$, for a fixed strength $K = 3.0$. It turns out that α_c decreases as the lattice becomes larger. The solid curve is a regression fit that enables us to extrapolate our results and estimate the value of α_c in the thermodynamical limit ($N \to \infty$), which turns

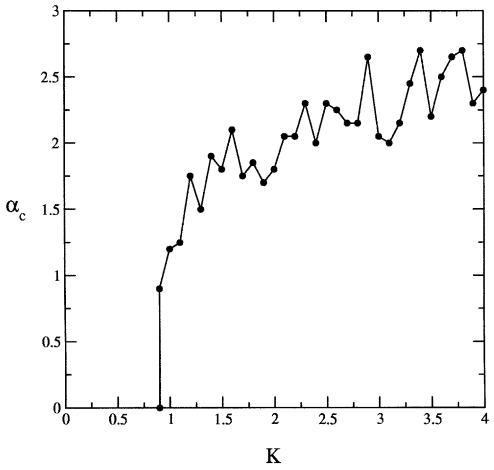

Fig. 5. Critical range parameter *versus* coupling strength.

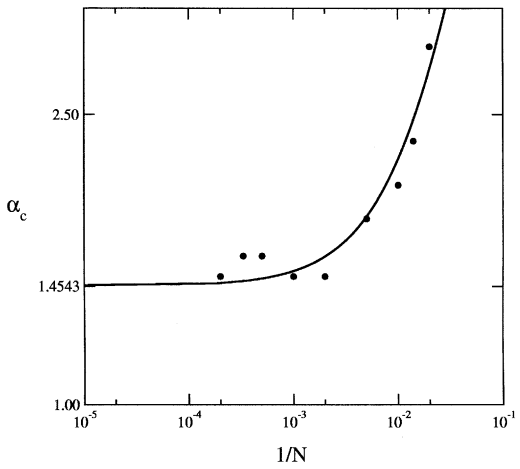

Fig. 6. Critical range parameter *versus* inverse lattice size for $K=3.0$. The solid line is a linear regression fit.

to be ≈ 1.45. In a previous paper [27] we have analyzed the large-N behavior of the statistical distribution of plateau lengths (in locally coupled map lattices) and found an exponential dependence.

4. Order parameter

In an oscillator chain, a completely phase-synchronized state is characterized by the equality of the oscillator phases for any time. Clusters of phase-synchronized oscillators

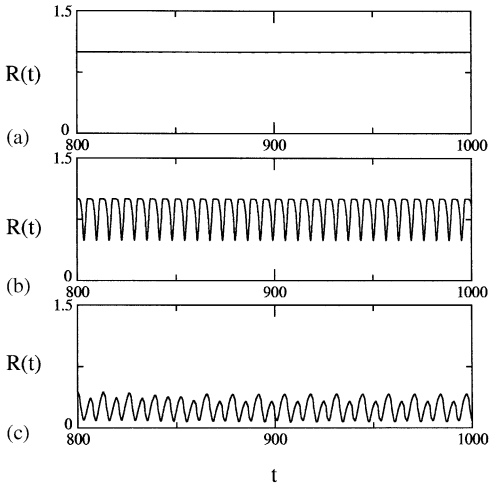

Fig. 7. Time series of the order parameter magnitude for a lattice of $N = 101$ vdP oscillators, with $K = 3.0$. (a) $\alpha = 0.0$; (b) $\alpha = 1.5$; and (c) $\alpha = 1.8$.

are defined in a similar way. Since phase synchronization always implies frequency synchronization, we would like to investigate in what extent the converse is true.

A useful diagnostic of phase synchronization is the complex order parameter introduced by Kuramoto [23]

$$z(t) = R(t)\exp[\mathrm{i}\varphi(t)] \equiv \frac{1}{N}\sum_{j=1}^{N}\exp[\mathrm{i}\theta^{(j)}(t)]\,. \tag{9}$$

The quantities $R(t) > 0$ and $\varphi(t) \in [0, 2\pi)$ are respectively the amplitude and angle of a gyrating vector which is equal to the vector sum of phasors for each oscillator in a lattice with periodic boundary conditions. Let us consider two extreme cases: firstly, with all sites having the same constant phase: $\theta^{(j)}(t) = \xi$, $(j = 1, 2, \ldots, N)$, i.e., a completely phase-synchronized state. The order parameter magnitude is $R(t) = 1$ for all times, with a constant argument $\varphi(t) = \xi$. For near phase-synchronized states, the order parameter magnitude $R(t)$ has a constant value near unity or either fluctuates around it.

On the other hand, let a pattern in which the site amplitudes $\theta^{(j)}(t)$ are so spatially uncorrelated that they can be considered as randomly distributed over the $[0, 2\pi)$ interval. Hence, we may regard the order parameter as the space-averaged factor

$$z(t) = \langle \mathrm{e}^{\mathrm{i}\theta^{(j)}(t)}\rangle_j = \langle\cos\theta^{(j)}(t)\rangle_j + \mathrm{i}\langle\sin\theta^{(j)}(t)\rangle_j = 0\,. \tag{10}$$

However, typical non-synchronized states are not completely uncorrelated in space, thus they exhibit a non-chaotic, yet very irregular oscillation about a *low* value of the order parameter magnitude.

Fig. 7(a) shows time series for the order parameter magnitude for some values of the range parameter. For global coupling R has a constant value very close to unity, that indeed characterizes a strongly phase-synchronized state. The order parameter oscillations for intermediate range [Fig. 7(b)] have amplitudes around $R = 1$ and

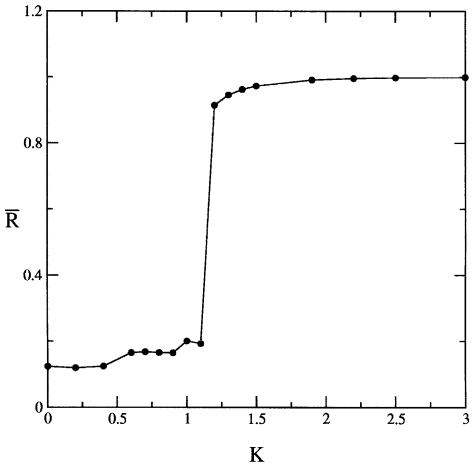

Fig. 8. Mean order parameter magnitude in terms of coupling strength for $\alpha = 0$.

exhibit periodic peaks, indicating abundance of phase-synchronized clusters. This behavior is typical for the frequency-synchronization transition depicted in Fig. 3. For $\alpha > \alpha_c$ [Fig. 7(c)], there are oscillations of $R(t)$ about small values, characterizing absence of phase synchronization.

The results depicted in Fig. 7 suggest that we shall focus on the temporal mean of the order parameter magnitude

$$\bar{R} = \lim_{t\to\infty} \frac{1}{t} \int_0^t R(t')\,\mathrm{d}t' \,. \tag{11}$$

Fig. 8 shows the dependence of $\bar{R}$ with the coupling strength for long effective range ($\alpha = 0$). The mean order parameter, which is initially small for weak coupling, jumps to its maximum value at $K = K_c \approx 1.2$, indicating that a transition between a non-synchronized regime and a phase-synchronized one has occurred. This is very similar to the situation illustrated by Figs. 4(a) and (b) for frequency synchronization. In fact, even the critical K value agrees with that obtained in the previous section. Hence, at least in this case, frequency synchronization implies phase synchronization, in agreement with the claims of Zheng and Hu [41].

This conclusion is not quite general, however, as exemplified by Fig. 9, where we plot the mean order parameter *versus* the coupling range, for a fixed strength. For long effective range we have phase synchronization ($\bar{R} = 1$), which disappears when α increases past $\alpha_c \approx 1.5$. As we would already expect, based on the frequency synchronization behavior, there is a transition as α increases, but the corresponding critical value is different (note that Fig. 3 indicates a value of about 1.7 for frequency synchronization). This suggests that in most situations phase and frequency synchronization appear together, but in the transitional region ($1.5 \lesssim \alpha \lesssim 1.7$) there may be cases in which the phases mismatch, while keeping their time rates unchanged, what yields frequency synchronization.

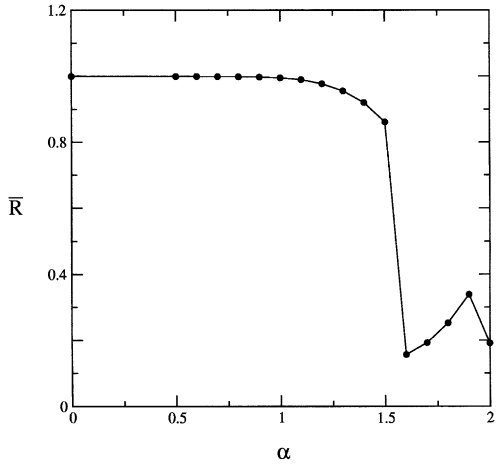

Fig. 9. Mean order parameter magnitude in terms of coupling range for $K = 3.0$.

The diversity of synchronization types exhibited by vdP oscillator chains may be observed in Fig. 10, where we present space–time plots of the x-variable for fixed K and different values of α. For global coupling [Fig. 10(a)] there is amplitude synchronization: $x^{(i)}(t) \approx x^{(j)}(t)$ for the entire lattice. Near the critical range [$\alpha = 1.7$, cf. Fig. 10(b)] the amplitudes for many sites exhibit lag synchronization $x^{(i)}(t) \approx x^{(j)}(t-\tau)$. This phenomenon has been intensively studied for chaotic systems [42]. A consequence of lag synchronization of a large number of sites with the same time delay is the presence of traveling waves. The propagation speed of the traveling wave is inversely proportional to the average delay $\langle\tau\rangle$ by which the oscillators are lagged from each other. For a range parameter slightly higher than its critical value [$\alpha = 1.9$, cf. Fig. 10(c)], we see two distinct sectors of the lattice presenting lag synchronization with *different* delays. Moreover, the time delays have opposite signs, so there are two traveling waves propagating through the lattice with opposite senses, and merging into a narrow region that looks like a kink–antikink pair. These rough boundaries between traveling wave trains form a kind of *synchronization defect* [43].

In Fig. 11, we fix α=0.0 and vary the coupling strength. An initially non-synchronized state for subcritical strength [$K = 1.10$, see Fig. 11(a)] evolves to a situation where we have both frequency and phase synchronization [Fig. 11(b)]. The latter case was obtained for $K = 1.15$, that is near the critical value of 1.2 indicated by Fig. 4. For higher K, we pass to an almost completely amplitude-synchronized state [Fig. 11(c)]. This strongly suggests that frequency and amplitude synchronization occur at any effective range. In summary, for α variations (fixed K) we observed that phase synchronization follows lag synchronization, but in the transitional region we can have frequency-synchronized states for which the phases are not synchronized [see Fig. 10]. On the other hand, for K variations (fixed α) frequency and amplitude/phase synchronization occur simultaneously [Fig. 11] [41].

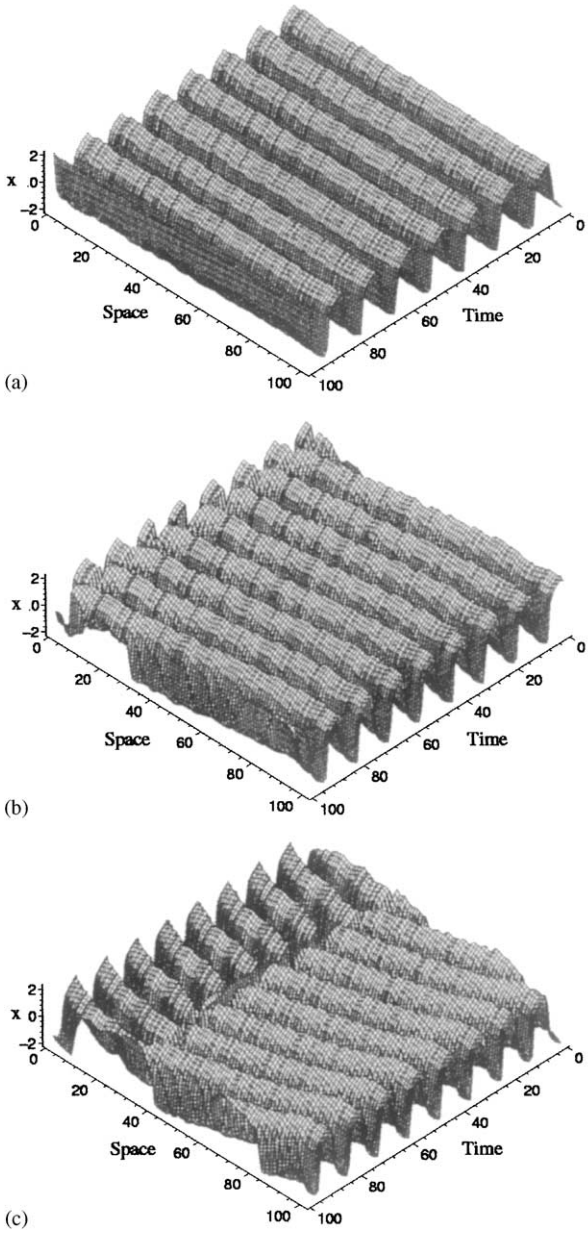

Fig. 10. Space–time plots of the x-amplitudes in a lattice with $N = 101$, $K = 3.0$. (a) $\alpha = 1.0$; (b) $\alpha = 1.7$; and (c) $\alpha = 1.9$. We plot 100 time steps after 900 transients.

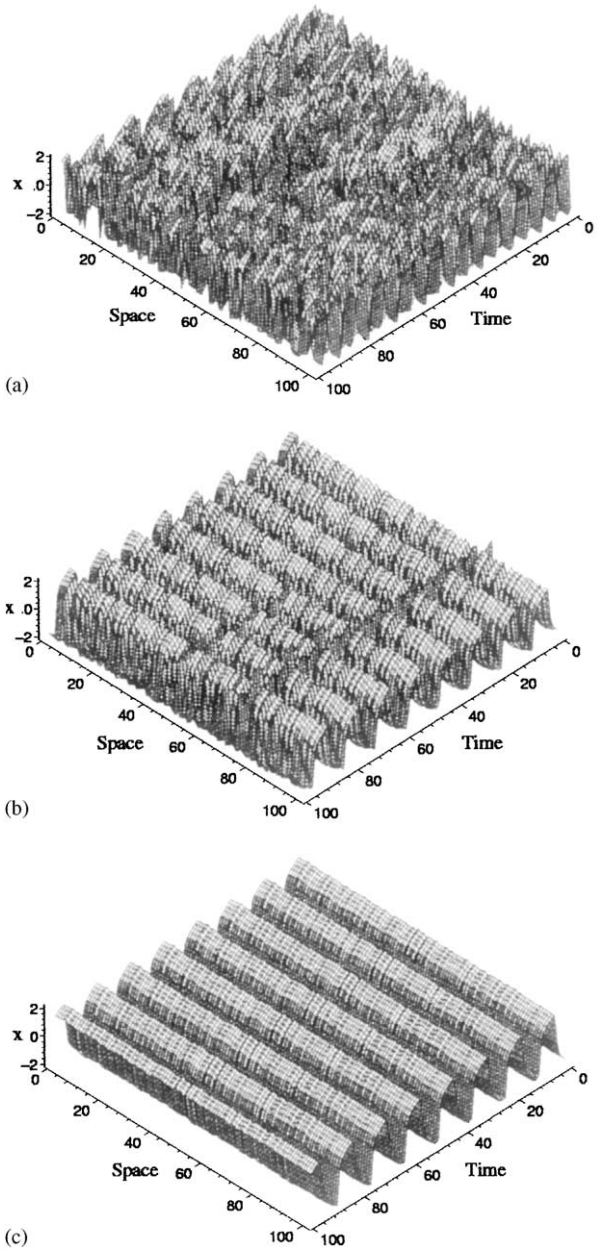

Fig. 11. Space–time plots of the x-amplitudes in a lattice with $N = 101$, $\alpha = 0.0$. (a) $K = 1.10$; (b) $K = 1.15$; and (c) $K = 3.00$. We plot 100 time steps after 900 transients.

5. Conclusions

The key to understand the mechanism whereby synchronization occurs in an oscillator chain is to consider the relative influences of coupling and disorder on the possible values of a state variable, phase, or frequency at each oscillator, depending on what is the synchronization type to be focused on. In particular, the distribution of the frequency synchronization plateaus is determined by the outcome of a competition between the diffusion effect of coupling and the frozen random disorder represented by the initially specified distribution of the normal mode frequencies over the lattice. The latter are chosen such that, if the oscillators are uncoupled, their frequencies are expected to have properties qualitatively similar to the normal modes themselves.

Frequency synchronization can occur if the coupling effect overcomes the frozen normal-mode randomness. For long effective range each site couples with many other sites, the relative intensity decreasing very slowly with the distance between the oscillators. Here the coupling effect is comparatively strong, and it easily overcomes the random disorder by making distant sites to adjust their frequencies and mutually synchronize. On the other hand, a local (short effective range) coupling connects only nearest neighbors in a significant way, its effect being too weak to make distant sites to synchronize and form a plateau. There is a transition between these limiting situations with a critical effective range that depends on the coupling strength and the lattice size. Coupled circle map lattices have shown values for the critical ranges smaller than those found for oscillator chains.

We have characterized the synchronization transition with variable effective range by using two diagnostics: the frequency dispersion around a space average and the average relative plateau size. The frequency synchronization transition observed when varying the effective range appears in both diagnostics and with slightly different critical values. We remark, however, that the average relative plateau size is a non-robust diagnostic in the sense that it is quite unstable and may lead sometimes to dubious results. Its use is only recommended in association with other diagnostics, like the frequency dispersion or the frequency order parameter proposed in Ref. [35].

Phase synchronization was characterized by analyzing the time behavior of the Kuramoto's order parameter magnitude. We observed that for global coupling it turns out that frequency synchronization implies phase synchronization (the converse is always true). For coupling regimes passing from global to local ones, in the transitional region we observed lag synchronization for one or more traveling waves propagating through the oscillator chain, what preserves frequency synchronization for a relatively large portion of the lattice. Although we have considered vdP oscillators in this paper, our results are also applicable to chains of more general limit-cycle oscillators, provided a phase and its corresponding frequency can be suitably defined.

Further work on this subject is still needed to understand the unpinning of the phase synchronized state that leads to lag synchronization. Moreover, the existence of traveling wave trains has led to a kind of synchronization defect. We conjecture that the production and interaction of these synchronization defects may desynchronize the

chain, in the same way as chaotic defects (resulting from two different zig-zag patterns) lead to defect turbulence [44].

Acknowledgements

This work was made possible by partial financial support from the following Brazilian government agencies: CNPq, CAPES, Fundação Araucária (State of Paraná), and FUNPAR (UFPR). The authors wish to thank Dr. Abraham Chian (INPE) for useful discussions and Dr. Alba Theumann (UFRGS) for pointing us the references on kinetic Ising models.

References

[1] P.S. Landa, Nonlinear Oscillations and Waves in Dynamical Systems, Kluwer Academic Publishers, Dordrecht, 1996.
[2] S.H. Strogatz, R.E. Mirollo, Physica D 31 (1988) 143.
[3] L.M. Pecora, T.L. Carroll, G.A. Johnson, D.J. Mar, J.F. Heagy, Chaos 7 (1997) 520.
[4] A. Winfree, The Geometry of Biological Time, Springer, New York, 1980.
[5] S.H. Strogatz, I. Stewart, Sci. Am. 68 (1993) 68.
[6] K. Wiesenfeld, P. Hadley, Phys. Rev. Lett. 62 (1989) 1335.
[7] A. Winfree, J. Theor. Biol. 16 (1967) 15.
[8] B. van der Pol, J. Van der Mark, Philos. Mag. 7 (1928) 763.
[9] L. Glass, P. Hunter, Physica D 43 (1990) 1.
[10] C.R. Katholi, F. Urthaler, J. Macy, T.N. Jones, Comput. Biomed. Res. 10 (1977) 529.
[11] J. Honerkamp, J. Math. Biol. 18 (1983) 69.
[12] J. Engelbrecht, O. Kongas, Appl. Anal. 57 (1995) 119.
[13] Y. Kuramoto, H. Nakao, Physica D 103 (1997) 294;
Y. Kuramoto, D. Battogtokh, H. Nakao, Phys. Rev. Lett. 81 (1998) 3543.
[14] S. Raghavachari, J.A. Glazier, Phys. Rev. Lett. 74 (1995) 3297.
[15] R. Kozma, Phys. Lett. A 244 (1998) 85.
[16] P.M. Gade, C.-K. Hu, Phys. Rev. E 60 (1999) 4966.
[17] D.J. Watts, S.H. Strogatz, Nature 393 (1998) 440.
[18] D.J. Watts, Small Worlds, Princeton University Press, Princeton, 1999.
[19] V.S. Afraimovich, V.I. Nekorkin, G.V. Osipov, V.D. Shalfeev, Stability, Structures and Chaos in Nonlinear Synchronization Networks, World Scientific, Singapore, 1994.
[20] G.V. Osipov, M.M. Sushchik, Phys. Rev. E 58 (1998) 7198.
[21] R.V. Jensen, Phys. Rev. E 58 (1998) R6907.
[22] T.E. Vadivasova, G.I. Strelkova, V.A. Anishchenko, Phys. Rev. E 63 (2001) 036225.
[23] Y. Kuramoto, Chemical Oscillations, Waves, and Turbulence, Springer, Berlin, 1984.
[24] S.H. Strogatz, Physica D 143 (2000) 1.
[25] J.L. Rogers, L.T. Wille, Phys. Rev. E 54 (1996) R2193.
[26] R.L. Viana, A.M. Batista, Chaos, Solitons Fractals 9 (1998) 1931.
[27] S.E. de Souza Pinto, R.L. Viana, Phys. Rev. E 61 (2000) 5154.
[28] A.M. Batista, S.E.S. Pinto, S.R. Lopes, R.L. Viana, Lyapunov spectrum and synchronization of piecewise linear map lattices with power-law coupling, Preprint (2001).
[29] K. Wiesenfeld, P. Colet, S.H. Strogatz, Phys. Rev. Lett. 76 (1996) 404.
[30] E. Ott, Chaos in Dynamical Systems, Cambridge University Press, Cambridge, 1994.
[31] J. Guckenheimer, P. Holmes, Nonlinear Oscillations, Dynamical Systems, and Bifurcations of Vector Fields, Springer, New York, 1983.
[32] G.V. Osipov, A.S. Pikowsky, M.G. Rosenblum, J. Kurths, Phys. Rev. E 55 (1997) 2353.

[33] A.S. Pikowsky, M.G. Rosemblum, G.V. Osipov, J. Kurths, Physica D 104 (1997) 219.
[34] A.C. Hindmarch, ODEPACK: a systematized collection of ODE solvers, in: R.S. Stepleman et al. (Eds.), Scientific Computing, North-Holland, Amsterdam, 1983, pp. 55;
L.R. Petzold, SIAM J. Sci. Statist. Comput. 4 (1983) 136.
[35] H. Sakaguchi, S. Shinomoto, Y. Kuramoto, Prog. Theor. Phys. 77 (1987) 1005.
[36] Gaveau, B. Gudowskanowak, R. Kapral, M.B. Moreau, Physica A 188 (1992) 443;
M. Bahiana, M.S.O. Massunaga, Phys. Rev. E 52 (1995) 321.
[37] A.M. Batista, R.L. Viana, Phys. Lett. A 286 (2001) 134.
[38] F. Schmüser, W. Just, H. Kantz, Phys. Rev. E 61 (2000) 3675.
[39] M.E. Fisher, S. Ma, B.G. Nickel, Phys. Rev. Lett. 29 (1972) 917;
M.E. Fisher, Rev. Mod. Phys. 46 (1974) 597.
[40] C. Boldrighini, L.A. Bunimovich, G. Cosimi, S. Frigio, A. Pellegrinotti, J. Statist. Phys. 102 (2001) 1271.
[41] Z. Zheng, G. Hu, Phys. Rev. E 62 (2000) 7882.
[42] M.G. Rosenblum, A.S. Pikowsky, J. Kurths, Phys. Rev. Lett. 78 (1997) 4193.
[43] A. Goryachev, R. Kapral, H. Chate, Int. J. Bifurcat. Chaos 10 (2000) 1537.
[44] K. Kaneko, in: K. Kaneko (Ed.), Theory and Applications of Coupled Map Lattices, Wiley, Chichester, 1993.